A theory of electromagnetically driven shock waves

By J. K. WRIGHT AND M. C. BLACK
Atomic Weapons Research Establishment, Foulness, Essex

(Received 5 December 1958)

During the last few years, many experimental devices have been built in which strong shock waves are generated in gases by electromagnetic forces on current-carrying gas particles. The general theory of these devices is discussed, taking external circuit inductance into account. It is shown that a shock wave of constant speed is finally attained. This shock wave is travelling at 90 % of its final speed when the circuit inductance has increased to 3·0 times its initial value.

1. Introduction

In recent years some attention has been directed towards producing strong shock waves in a gas by means of a technique known as electromagnetic driving. The apparatus used may take a variety of forms but the basic principles are very similar. Figure 1 (*a*) shows a simple arrangement as used, for example, by Kolb (1957). A low inductance condenser bank is discharged between two electrodes in a gas. The return path is close to the discharge and the electromagnetic interaction between them drives the current-carrying gas particles away from the return lead with such a force that an intense shock wave is produced.

The electromagnetic forces can be considered in various equivalent ways. One method is to treat the current in the gas as being in the magnetic field due to the current in the return path, but a more convenient approach from our point of view is to look upon the magnetic field H as exerting a pressure $H^2/8\pi$ normal to the field and a tension $H^2/8\pi$ in the direction of the field on the current-carrying gas particles. (Here and throughout this paper the electromagnetic system of units is employed.) In our case the motion is normal to the direction of the field and the hydrodynamics of the gas can therefore be analysed by assuming that the current sheet is forced forwards by a piston exerting a pressure $H^2/8\pi$, and in fact the magnetic field is often said to act as a 'magnetic piston'. Another possible apparatus for generating strong shocks is depicted in figure 1 (*b*). Here the currents in the gas are confined to a cylindrical sheet which is driven inwards under the action of the circumferential magnetic field. At low ambient gas pressures, a stream of high energy particles is driven towards the axis and this is the basis of the various high-speed pinch devices that have been reported by Artsimovich *et al.* (1956), Anderson *et al.* (1957), Bodin & Reynolds (1957), and Hagerman & Mather (1958). At higher gas pressures, collisions occur between the accelerated particles and the relatively stationary particles ahead of them and an imploding shock wave is produced.

It is also possible to produce a cylindrically imploding shock by the electrodeless discharge arrangement shown in figure 1 (*c*). When the switch is closed, a current starts to flow in the circuit round the discharge tube. The consequent electric field induced in the gas is greatest at the walls and a current flows in the opposite direction to the primary current. In this case the current paths are

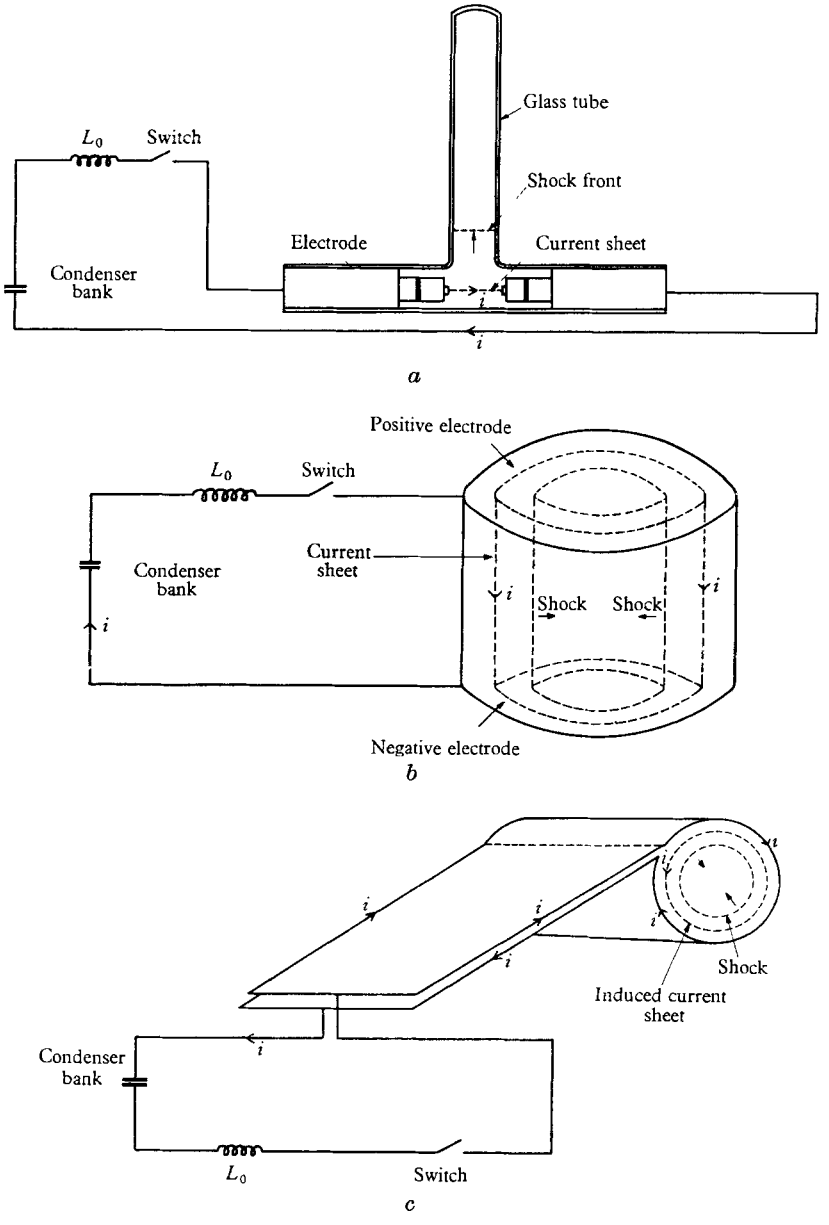

FIGURE 1. Various experimental arrangements for the production of strong shock waves using electromagnetic driving. In each of the arrangements the magnetic field produced by the discharge acts on the current-carrying gas particles which are driven under the action of the Lorentz force.

circumferential and the gas particles are driven inwards by the longitudinal magnetic field. This is the basis of the device reported by Elmore, Little & Quinn (1958).

Although the three practical arrangements differ from each other in their geometrical patterns, when the discharge is first formed the effect of the cylindrical convergence in the cases shown in figures 1 (*b*) and 1 (*c*) is negligible, and we may obtain results applicable to all three devices by analysis of the simple arrangement shown in figure 2. This consists of two parallel plane electrodes of breadth a a distance b apart. When the switch is closed the gas breaks down and currents flow along the path of minimum inductance, i.e. close to the return path. This situation has been analysed by Allen (1957), who assumed that (*a*) the conductivity of the circuit is infinite, (*b*) the thickness of the shock wave is small compared with the dimensions of the discharge chamber, and (*c*) the current rises instantaneously from zero to a finite value and then remains constant.

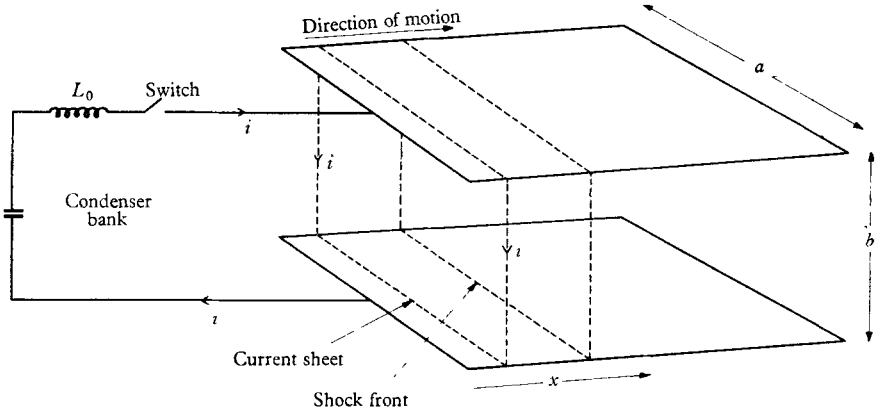

FIGURE 2. A simple one-dimensional model of the electromagnetically driven shock wave apparatus.

In practice there will be a finite time before the steady-state condition (*c*) is attained since the external circuit will have a finite inductance L_0, even initially when the current in the gas chooses the path for which this inductance is a minimum. It is the purpose of this investigation to determine the time taken for the current to build up to its steady value and the effect of the formation time on the structure of the generated shock wave.

In § 2 we discuss the equations of motion of the conducting gas and the relevant boundary conditions, putting them in a non-dimensional form convenient for analysis. In § 3 we consider the phenomena occurring at a very early stage in the discharge. Here the circuit inductance has risen from L_0 to $L_0 + L$ and we assume L to be negligible compared with L_0. This gives a very convenient similarity solution, which is improved upon in § 4 by including L in the equations and using Taylor series expansions. The expansions are applicable, however, only so long as τ, a non-dimensional time, is small. We use this solution as a starting-point for the solution of the whole flow, obtained by the method of characteristics, and this is described in § 5. The results are discussed in § 6.

2. Basic theory

In our system we have three regions. First of all there is the gas ahead of the shock front which is in its ambient non-ionized condition. There is no magnetic field in this region. Then there is the region of shocked gas where again there is no magnetic field. The boundary conditions between the first and second regions are the normal Rankine–Hugoniot relations for a gas in the absence of a magnetic field. Finally there is the third region where there is no gas but a magnetic field H. There is a current sheet in the gas at the boundary between regions two and three and the boundary conditions equate magnetic pressure in region three with hydrodynamic pressure in region two.

Using Lagrangian co-ordinates, we formulate the equations of motion and boundary conditions of the conducting gas. Let s be the Lagrangian co-ordinate of a particle, and x be the position of that particle at time t. We denote by u, p and ρ the particle speed, pressure, and density at the point (s, t). The gas is initially at rest with density ρ_0.

Equations of motion of the gas

The equations of conservation of mass and momentum are

$$\rho \frac{\partial x}{\partial s} = \rho_0, \tag{2.1}$$

$$\rho \frac{\partial u}{\partial t} = -\frac{\partial p}{\partial x}. \tag{2.2}$$

Using (2.1) and $\frac{\partial p}{\partial x} = \frac{\partial p}{\partial s} \Big/ \frac{\partial x}{\partial s}$ we rewrite (2.2) as

$$\rho_0 \frac{\partial u}{\partial t} = -\frac{\partial p}{\partial s}. \tag{2.3}$$

Once the element of gas with co-ordinate s has been shocked, all further changes at this element are isentropic. This gives a third equation of motion

$$\frac{\partial}{\partial t}(p\rho^{-\gamma}) = 0, \tag{2.4}$$

where for a fully ionized gas, $\gamma = \frac{5}{3}$.

Boundary conditions at the shock

At the shock front we have the boundary conditions

$$x = s, \tag{2.5}$$

and

$$\frac{ds}{dt} = U, \tag{2.6}$$

where U is the velocity of the shock.

We assume that the magnetic pressure is at all times much greater than the ambient pressure so that the Rankine–Hugoniot relations for a singly ionized gas take the simple 'strong shock' form,

$$\rho = 4\rho_0, \tag{2.7}$$

$$u = \tfrac{3}{4}U, \tag{2.8}$$

$$p = \tfrac{4}{3}\rho_0 u^2. \tag{2.9}$$

In these equations, allowance has been made for the partial pressure of the electrons which are supposed to be in thermal equilibrium with the ions, and the ionization and dissociation energies are supposed negligible compared with the thermal energy of the gas.

Boundary conditions at the current sheet

At the current sheet we may equate the magnetic pressure $H^2/8\pi$ outside the gas with the hydrodynamic pressure inside, giving

$$p = \frac{H^2}{8\pi}.$$

H is related to the current i in the discharge, and we may write

$$p = \frac{2\pi i^2}{a^2}. \tag{2.10}$$

When the low impedance current source at a constant potential V_0 is connected to the circuit of negligible resistance and constant inductance L_0, the discharge voltage is given by

$$V = V_0 - L_0 \frac{di}{dt}. \tag{2.11}$$

We also have

$$V = \frac{d}{dt}(Li). \tag{2.12}$$

Equating (2.11) with (2.12), we have

$$L_0 \frac{di}{dt} + \frac{d}{dt}(Li) = V_0,$$

which integrates to

$$(L_0 + L)\, i = V_0 t. \tag{2.13}$$

The inductance of the discharge circuit in the gas, L, is directly proportional to the distance x that the current sheet has travelled, and if the inductance L becomes equal to L_0 at a distance $x = x_0$ we may write $L/L_0 = x/x_0$ and hence equation (2.13) may be written

$$L_0\left(1 + \frac{x}{x_0}\right) i = V_0 t. \tag{2.14}$$

Eliminating i from (2.10) and (2.14), we obtain

$$p\left(1 + \frac{x}{x_0}\right)^2 = \frac{2\pi}{a^2} \frac{V_0^2}{L_0^2} t^2. \tag{2.15}$$

Equation (2.15) gives the boundary condition to be satisfied at the piston, whose Lagrangian co-ordinate is

$$s = 0. \tag{2.16}$$

Since the current takes some time to build up in the discharge, the initial magnetic pressure is very small, but as a consequence of our assumption that the shock pressure is much greater than the ambient pressure, a particle close to the current sheet that has just been shocked will have $\rho = 4\rho_0$ by equation (2.7). Since the pressure increases as the discharge current builds up, this gas particle is

compressed isentropically and its density increases. In the limit, at the current path, we may write

$$s = 0, \quad \rho = \infty. \tag{2.17}$$

We now reduce the equations of motion to a non-dimensional form by the following substitutions:

$$\left.\begin{aligned} \frac{x}{x_0} &= \xi, \quad \frac{s}{x_0} = \alpha, \quad \frac{\rho}{\rho_0} = D, \quad \frac{u}{u^*} = v \\ \frac{U}{u^*} &= w, \quad \frac{u^* t}{x_0} = \tau, \quad \frac{p}{\rho_0 (u^*)^2} = P, \end{aligned}\right\} \tag{2.18}$$

where

$$(u^*)^4 = \frac{V_0^2}{8\pi\rho_0 b^2}. \tag{2.19}$$

Equations (2.1), (2.3) and (2.4) become

$$D\frac{\partial \xi}{\partial \alpha} = 1, \tag{2.20}$$

$$\frac{\partial v}{\partial \tau} = \frac{\partial P}{\partial \alpha}, \tag{2.21}$$

$$\frac{\partial}{\partial \tau}(PD^{-\gamma}) = 0. \tag{2.22}$$

The boundary conditions at the shock, (2.5) to (2.9), become

$$\left.\begin{aligned} \xi &= \alpha, \quad \frac{d\alpha}{d\tau} = w, \\ D &= 4, \quad v = \tfrac{3}{4}w, \quad P = \tfrac{4}{3}v^2. \end{aligned}\right\} \tag{2.23}$$

The boundary conditions at the piston, (2.15) to (2.17), become

$$P(1+\xi)^2 = \tau^2, \quad \alpha = 0, \quad D = \infty. \tag{2.24}$$

3. Similarity solution at early times

In the initial stages we may neglect L compared with L_0. This has the effect of changing the first of the boundary conditions (2.24) at the piston to

$$P = \tau^2. \tag{3.1}$$

We now obtain our equations in terms of a new variable $\eta = \alpha/\tau^2$.

Let

$$P = \tau^2 P_1(\eta), \tag{3.2}$$

$$\xi = \tau^2 \xi_1(\eta), \tag{3.3}$$

$$D = D_1(\eta) \tag{3.4}$$

Equations (2.20) to (2.22) become

$$D_1 \frac{d\xi_1}{d\eta} = 1, \tag{3.5}$$

$$4\eta^2 \frac{d^2\xi_1}{d\eta^2} - 2\eta\frac{d\xi_1}{d\eta} + 2\xi_1 = -\frac{dP_1}{d\eta}, \tag{3.6}$$

$$\frac{d}{d\eta}\left\{\frac{P_1 D_1^{-\gamma}}{\eta}\right\} = 0. \tag{3.7}$$

If the position of the shock is $\eta = \beta$, i.e. $\alpha = \tau^2\beta$, then the speed of the shock is $w = d\alpha/d\tau = 2\tau\beta$, and $v = \frac{3}{4}w = \frac{3}{2}\tau\beta$. Thus the boundary conditions at the shock become

$$\xi_1 = \eta = \beta, \quad D_1 = 4, \quad P_1 = 3\beta^2. \tag{3.8}$$

The boundary conditions at the piston become

$$P_1 = 1, \quad \eta = 0, \quad D_1 = \infty. \tag{3.9}$$

We may integrate (3.7) and use the boundary conditions at the shock, giving

$$P_1 = 3\beta\eta\left(\frac{D_1}{4}\right)^{\gamma}. \tag{3.10}$$

Equations (3.5), (3.6) and (3.10) can be integrated numerically, giving

$$\beta = 0{\cdot}449 \quad \text{and} \quad [\xi_1]_{\eta=0} = -0{\cdot}388.$$

4. Taylor series extension

The solution in §3 is now extended using a Taylor series expansion, thus enabling us to correct for the boundary condition $P(1+\xi)^2 = \tau^2$.

Put

$$\xi = \tau^2\xi_1(1+A\tau^2), \tag{4.1}$$

$$P = \tau^2 P_1(1+B\tau^2), \tag{4.2}$$

$$D = D_1(1+C\tau^2), \tag{4.3}$$

where A, B, and C are functions of η. Terms involving higher orders of τ are negligible for values of $\tau < 0{\cdot}35$.

Equations (2.20) and (2.21) become

$$R - C\frac{d\xi_1}{d\eta} = 0, \tag{4.4}$$

$$4\eta^2\frac{d^2R}{d\eta^2} - 10\eta\frac{dR}{d\eta} + 12R + \frac{dS}{d\eta} = 0, \tag{4.5}$$

where $R = A\xi_1$, $S = BP_1$, and equation (2.22) integrates to

$$PD^{-\gamma} = f(\alpha) \tag{4.6}$$

In our similarity solution we showed that when L is negligible (4.6) becomes

$$f(\alpha) = \frac{3\beta}{4^{\gamma}}\alpha. \tag{4.7}$$

We therefore apply a Taylor series expansion and write (4.6) in the extended case as

$$PD^{-\gamma} = \frac{3\beta}{4^{\gamma}}\alpha(1+q\alpha), \tag{4.8}$$

where q is a constant and terms of $O(\alpha^3)$ are neglected. Substituting for P and D from (4.2) and (4.3), we obtain

$$S = P_1(\gamma C + q\eta). \tag{4.9}$$

The new shock position is then

$$\alpha_s = \beta\tau^2(1+E\tau^2). \tag{4.10}$$

At the shock we have

$$\xi_s = \tau^2 \xi\left(\frac{\alpha_s}{\tau^2}\right)(1 + A\tau^2), \tag{4.11}$$

$$P_s = \tau^2 P\left(\frac{\alpha_s}{\tau^2}\right)(1 + B\tau^2), \tag{4.12}$$

$$D_s = D\left(\frac{\alpha_s}{\tau^2}\right)(1 + C\tau^2). \tag{4.13}$$

Equations (4.11) to (4.13) are expanded using (4.10), and our boundary conditions at the shock (2.23) become

$$A = \tfrac{3}{4}E, \quad B = \tfrac{39}{8}E, \quad C = \tfrac{9}{8}E. \tag{4.14}$$

The boundary conditions at the piston (2.24) become

$$S = -2[\xi_1]_{\eta=0}, \quad C = -\tfrac{6}{5}[\xi_1]_{\eta=0}. \tag{4.15}$$

Equations (4.4), (4.5) and (4.9), which are now no longer functions of η alone, can be integrated numerically for a particular value of τ, giving

$$\tau = 0{\cdot}35, \quad E = -0{\cdot}144, \quad \alpha_s = 0{\cdot}054, \quad q = -0{\cdot}981.$$

5. Solution by characteristics

The solution is now completed using the method of characteristics. From (2.20) and (2.21) we obtain the following relations which are used in finite difference form:

$$\delta v - \frac{1}{\sqrt{(\gamma PD)}}\delta P = 0 \quad \text{along} \quad \frac{d\alpha}{d\tau} = -\sqrt{(\gamma PD)}, \tag{5.1}$$

$$\delta v + \frac{1}{\sqrt{(\gamma PD)}}\delta P = 0 \quad \text{along} \quad \frac{d\alpha}{d\tau} = \sqrt{(\gamma PD)}. \tag{5.2}$$

The Taylor series expanded similarity solution may now be used as a starting-point for the numerical integration along the characteristics given by (5.1) and (5.2). This integration was carried out on the A.W.R.E. I.B.M. 704 computor until a shock wave of constant speed was attained.

6. Discussion of results

The position of the shock front and current sheet as a function of time are depicted in figure 3. The curves which are initially parabolic (similarity solution) tend asymptotically to straight lines when the steady state has been attained. Values of the non-dimensional hydrodynamic parameters at the shock front and current sheet are tabulated in table 1. The shock speed w has been calculated as a function of the final steady velocity attained w_f and the result is plotted in figure 4. It will be seen that the shock has achieved 90 % of its final speed after it has travelled a non-dimensional distance 2·5 in a non-dimensional time 3·1. At this time the current sheet has travelled a distance 2·0 units and the total inductance of the system has therefore risen from L_0 to $3{\cdot}0L_0$. We may therefore conclude that the constant current approximation of Allen becomes valid when

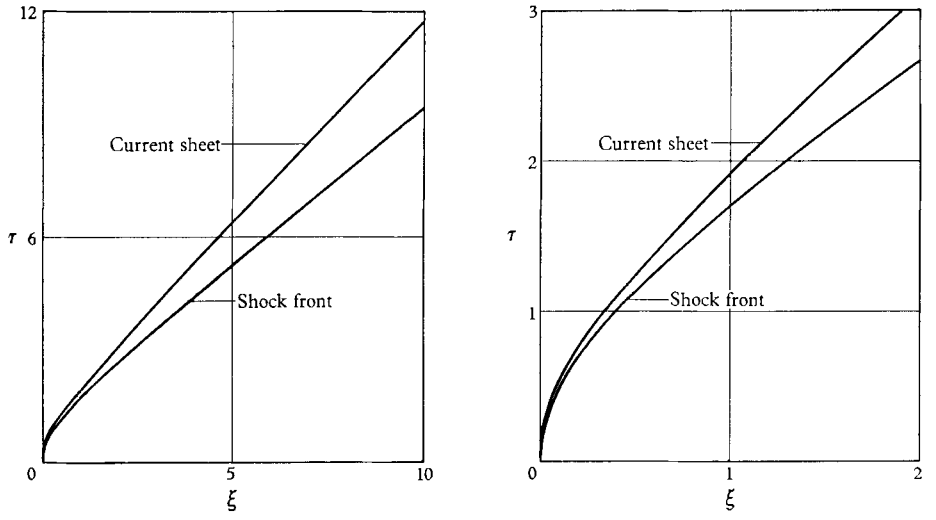

FIGURE 3. Distance–time plot showing the motion of shock front and current sheet. ξ is a non-dimensional distance and τ is a non-dimensional time.

Piston						Shock				
τ	ξ	P	v	V/V_0	$i/i_{\max}$	ξ	P	v	w	w/w_f
0·05	0·00097	0·00250	0·0384	0·003	0·046	0·00112	0·00151	0·0337	0·0449	0·036
0·10	0·00387	0·00992	0·0767	0·012	0·093	0·00448	0·00601	0·0671	0·0895	0·072
0·15	0·00869	0·0221	0·114	0·025	0·138	0·0101	0·0134	0·0995	0·133	0·107
0·20	0·0154	0·0388	0·152	0·045	0·183	0·0179	0·0236	0·132	0·176	0·142
0·25	0·0240	0·0596	0·188	0·068	0·227	0·0279	0·0364	0·165	0·220	0·177
0·30	0·0343	0·0841	0·225	0·096	0·270	0·0400	0·0515	0·197	0·263	0·212
0·35	0·047	0·112	0·260	0·128	0·311	0·054	0·069	0·227	0·303	0·244
0·40	0·060	0·142	0·295	0·162	0·351	0·070	0·088	0·257	0·343	0·276
0·45	0·076	0·175	0·329	0·199	0·389	0·088	0·110	0·287	0·383	0·309
0·5	0·093	0·209	0·359	0·235	0·426	0·108	0·132	0·315	0·420	0·338
0·6	0·13	0·28	0·42	0·312	0·494	0·15	0·18	0·37	0·49	0·395
0·7	0·18	0·36	0·47	0·389	0·552	0·21	0·23	0·42	0·56	0·451
0·8	0·23	0·43	0·52	0·462	0·605	0·27	0·28	0·46	0·62	0·500
0·9	0·28	0·49	0·56	0·527	0·654	0·33	0·33	0·50	0·67	0·540
1·0	0·34	0·56	0·60	0·588	0·696	0·40	0·39	0·54	0·72	0·580
1·2	0·47	0·67	0·66	0·686	0·762	0·55	0·48	0·60	0·80	0·645
1·4	0·60	0·77	0·72	0·769	0·817	0·72	0·56	0·65	0·87	0·701
1·6	0·75	0·84	0·76	0·826	0·853	0·90	0·64	0·69	0·92	0·741
1·8	0·91	0·89	0·79	0·866	0·878	1·09	0·71	0·73	0·97	0·782
2·0	1·1	0·93	0·81	0·891	0·897	1·3	0·75	0·75	1·00	0·806
2·5	1·5	1·02	0·85	0·940	0·940	1·8	0·85	0·80	1·07	0·862
3·0	1·9	1·06	0·88	0·969	0·958	2·4	0·92	0·83	1·11	0·895
4·0	2·8	1·10	0·90	0·986	0·976	3·5	1·01	0·87	1·16	0·935
5·0	3·7	1·12	0·92	0·995	0·984	4·7	1·06	0·89	1·18	0·951
10·0	8·3	1·15	0·93	1·000	0·998	10·7	1·11	0·91	1·22	0·983

TABLE 1

the inductance of the system has increased to the order of three times its initial value.

When the steady state has been attained, the distance–time relationships for the piston and shock tend to the lines

$$\xi = 0{\cdot}93\tau - 1{\cdot}0, \tag{6.1}$$

and

$$\xi = 1{\cdot}24\tau - 1{\cdot}3, \tag{6.2}$$

corresponding to non-dimensional speeds of 0·93 and 1·24 respectively. Returning to our original physical units, we get final piston and shock speeds given by

$$u = 0{\cdot}416\left\{\frac{V_0^2}{\rho_0 b^2}\right\}^{\frac{1}{4}}, \quad U = 0{\cdot}554\left\{\frac{V_0^2}{\rho_0 b^2}\right\}^{\frac{1}{4}}. \tag{6.3}$$

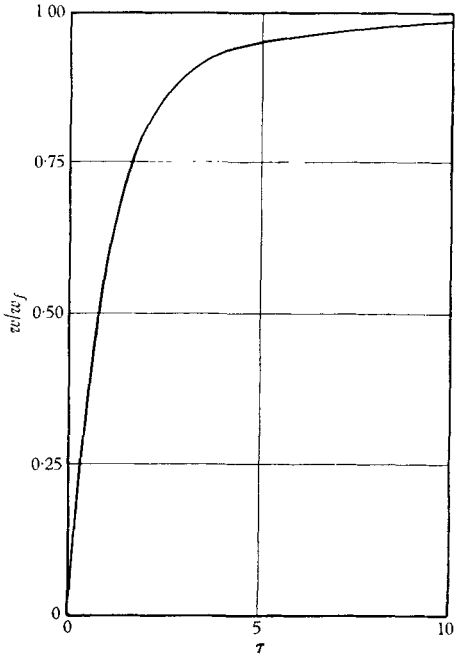

FIGURE 4. Shock speed as a function of time. w/w_f is the shock speed expressed as a ratio of that finally attained, and τ is a non-dimensional time.

The variation of voltage V across the discharge and current i as a function of time can be determined from the boundary conditions at the piston, equations (2.13) and (2.11). We obtain

$$i = \frac{V_0 x_0 \tau}{L_0 u^*(1+\xi)}, \quad V = V_0\left\{\frac{v\tau + \xi + \xi^2}{(1+\xi)^2}\right\}. \tag{6.4}$$

The values of V/V_0 and $i/i_{\max}$ are presented in table 1 and plotted as a function of time in figures 5 and 6.

We now consider the variations of pressure, density, temperature and particle speed in the gas with distance at various values of time. Typical results are presented in figure 7. It will be seen that the density rises rapidly towards the

piston. This is because a particle of gas that is initially close to the origin is compressed to 4 times its initial density by a relatively weak shock. As the current rises in the discharge, the pressure increases and this particle is compressed to a high density. At early stages of the discharge ($\tau = 0{\cdot}1$, $0{\cdot}35$) the current is rising rapidly and the variation in density extends as far as the shock front, whereas at late stages ($\tau = 10{\cdot}0$) there is a layer of almost constant density behind the shock front before the thin highly compressed layer at the current sheet.

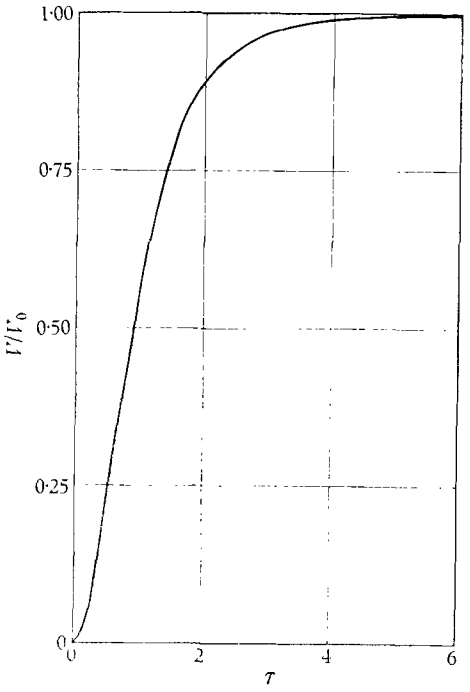

FIGURE 5

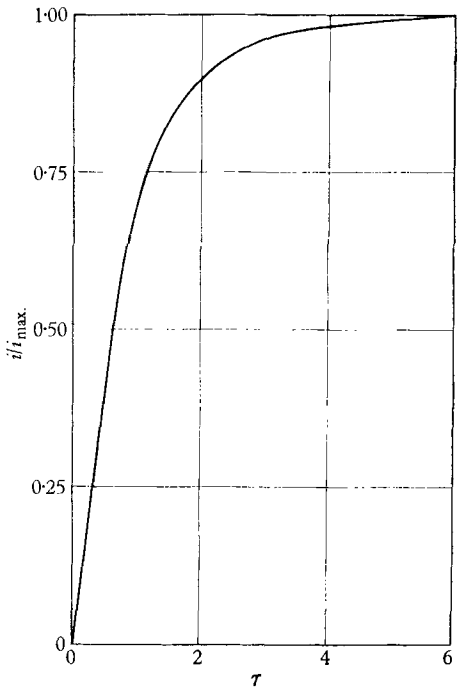

FIGURE 6

FIGURE 5. Voltage across the discharge as a function of time. V/V_0 is the discharge voltage compared with the source voltage, and τ is a non-dimensional time.

FIGURE 6. Discharge current as a function of time. i is the discharge current at non-dimensional time, τ, and i_{max} is the current when the shock has attained a constant speed.

At early stages in the discharge the pressure at the shock front is only 60 % of that at the current sheet. This is because the mass of shocked gas is being accelerated rapidly and there is therefore a large pressure gradient in the gas. As the steady state is gradually attained, the acceleration of the shocked gas falls off and the pressure gradient disappears. Thus, at time $\tau = 10$, the pressure at the shock is 96 % of that at the current sheet.

The variation in temperature in the gas can be easily interpreted since it is proportional to pressure divided by density. At early stages there is a fall in temperature all the way back from the shock front, whereas at late stages we have a region of fairly uniform temperature close to the shock front and a cold slab of gas close to the current sheet. It should be mentioned at this point that all the preceding analysis has assumed that the rate of energy transfer between points

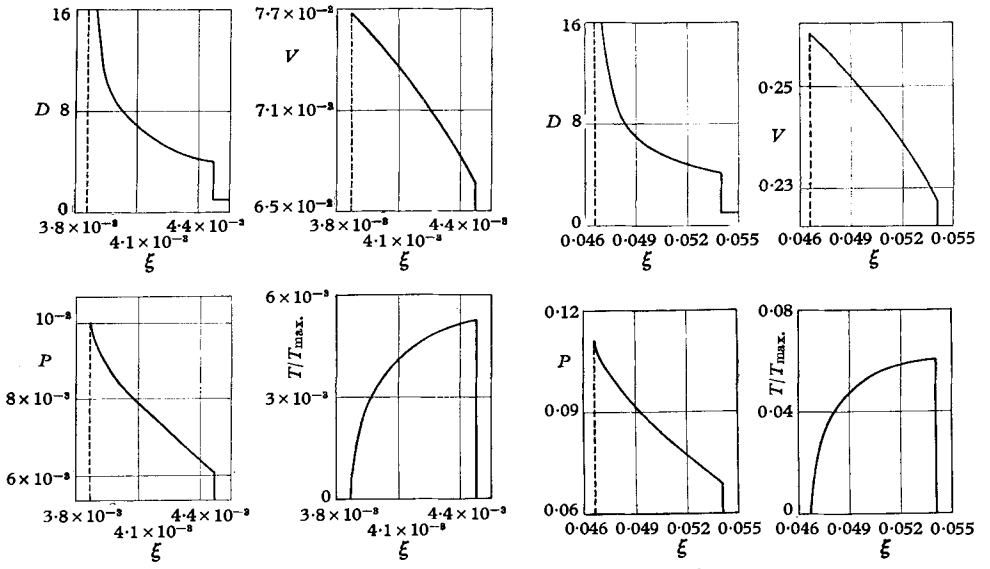

(a) $\tau = 0{\cdot}1$ (b) $\tau = 0{\cdot}35$

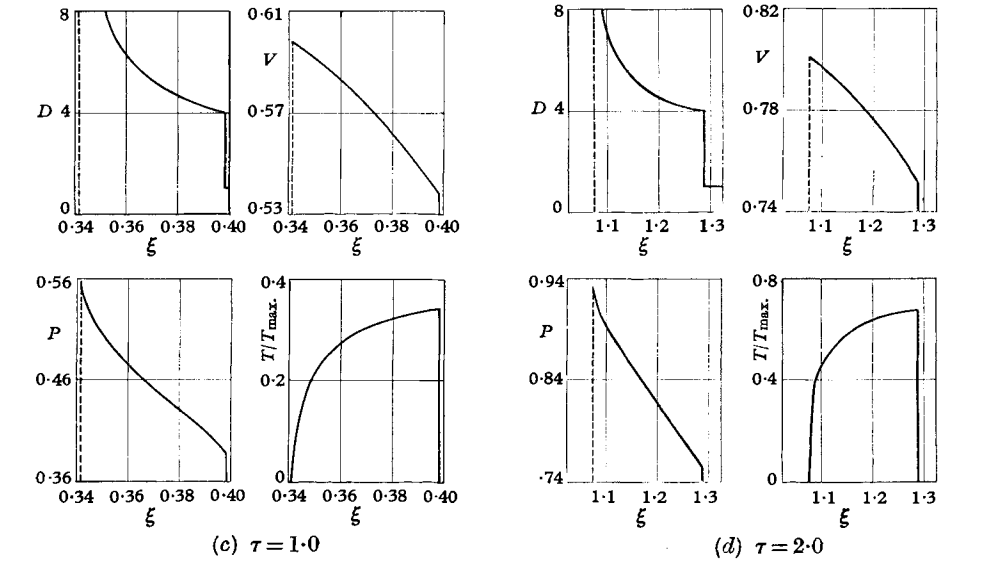

(c) $\tau = 1{\cdot}0$ (d) $\tau = 2{\cdot}0$

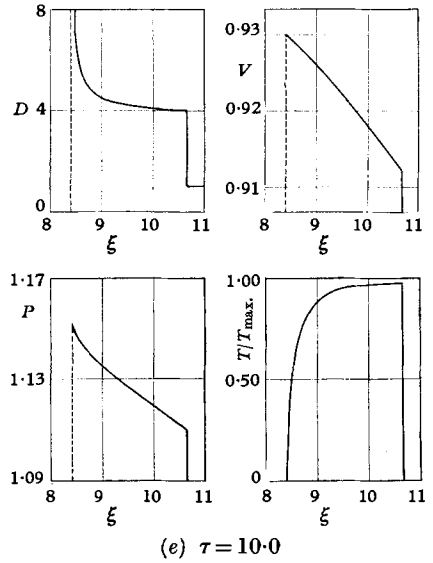

(e) $\tau = 10{\cdot}0$

FIGURE 7. Hydrodynamic parameters in the shocked plasma as a function of non-dimensional distance ξ for various values of the non-dimensional time τ.

in the gas by means of thermal conduction is negligible. In practice the thermal conductivity may be very high and, in applying the results of this paper to specific practical cases, it is necessary to satisfy oneself that this basic assumption is valid.

It will be noticed that at all times the particle speed v is remarkably uniform across the gas. This is because at early stages, when the current is rising rapidly, the time taken for sound waves to traverse the gas is very small and local compressions with associated variations in particle speed do not have time to develop.

Finally we return to our initial assumption of a fully ionized and dissociated gas with the ionization and dissociation energies negligible compared with the thermal energy of the gas. In order to completely ionize and dissociate hydrogen, deuterium or tritium, it is necessary to put in 15 eV of energy per atom present. The above assumption is therefore only valid when the thermal energy of the gas is large compared with this energy, i.e. the temperature of the gas must be much greater than $1{\cdot}7 \times 10^5$ °K. Since the similarity solution (§ 3) gives a shock strength (and therefore temperature) increasing as the square of time, there is a finite time before this condition is attained.

REFERENCES

Allen, J. E. 1957 An elementary theory of the transient pinched discharge. *Proc. Phys. Soc.* B, **70**, 24.

Anderson, D. A., Baker, W. R., Colgate, S., Gilbert, F. C., Ise, J., Pyle, R. V. & White, R. S. 1957 Paper presented at conference on Plasma Physics, Venice.

Artsimovich, L. A., Andrianov, A. M., Bazilevskaya, O. A., Prokhorov, Yu. G. & Filippov, N. V. 1956 *Atomnaya Energiya*, **3**, 76.

Bodin, H. A. B. & Reynolds, J. A. 1957 *Engineering*, **184**, 538.

Elmore, W. C., Little, E. M. & Quinn, W. E. 1958 Neutrons of possible thermonuclear origin. *Phys. Rev. Letters*, **1**, 32.

Hagerman, D. C. & Mather, J. W. 1958 Neutron production in a high power pinch apparatus. *Nature, Lond.*, **181**, 226.

Kolb, A. C. 1957 Production of high energy plasmas by magnetically driven shock waves. *Phys. Rev.* **107**, 345.